# Interaction parameters of poly(vinyl methyl ether) in aqueous solution as determined by small-angle neutron scattering

**K. Okano**
*Faculty of Education, Shinshu University, Nishinagano, Nagano 380, Japan*

**and M. Takada* and K. Kurita**
*Department of Industrial Chemistry, College of Science and Technology, Nihon University, Chiyoda-ku, Tokyo 101, Japan*

**and M. Furusaka**
*National Laboratory for High Energy Physics, Tsukuba, Ibaraki 305, Japan*
*(Received 22 September 1993; revised 20 October 1993)*

We have measured the small-angle neutron scattering from semidilute solutions of poly(vinyl methyl ether) in water and in methanol–water mixtures in a poor solvent regime. The binary and ternary cluster integrals of the polymer segments were determined from the concentration dependence of the correlation length at various temperatures just below the lower critical solution temperature. We have calculated the contributions of the segment–segment interactions to the entropy and enthalpy from the measured temperature dependences of these interaction parameters and found that both quantities are positive and decrease with increasing methanol content. The implication of these findings is discussed.

**(Keywords: interaction parameter; poly(vinyl methyl ether); small-angle neutron scattering)**

## INTRODUCTION

Poly(vinyl methyl ether) (PVME) is an amphiphilic polymer and is soluble both in water and in some organic solvents; its aqueous solution has a lower critical solution temperature (*LCST*), while in cyclohexane it shows an upper critical solution temperature (*UCST*).

In this work we are concerned with the effective segment–segment interactions of PVME in an aqueous medium, which are considered to comprise the effects of hydrogen bonding between the ether groups of PVME and water molecules as well as the effects of hydrophobic hydration around the apolar groups of PVME. It is also of interest to know how the addition of alcohol molecules to the aqueous solvent modifies the effective segment–segment interactions of PVME.

For these purposes we measured the small-angle neutron scattering (SANS) from semidilute solutions of PVME in water and in methanol–water mixtures having different compositions. From the angular dependence of the scattered intensity we were able to determine the binary and ternary cluster integrals of the polymer segments for each solution.

We extracted from these interaction parameters the contributions of the segment–segment interactions to the entropy $S_{\mathrm{int}}$ and the enthalpy $U_{\mathrm{int}}$. It turned out that both $S_{\mathrm{int}}$ and $U_{\mathrm{int}}$ are positive for an aqueous solution and also for solutions of methanol–water mixtures contrary to the case of the usual *UCST* system, e.g. the PVME–cyclohexane system. The cause of this anomalous behaviour will be discussed.

## SMALL-ANGLE NEUTRON SCATTERING

### *Semidilute poor solvent solution and scattering law*

We consider a semidilute polymer solution in which the volume fraction of polymer chains is small but the chains fully overlap one another.

Semidilute solutions at a given temperature can be classified into three regimes: good, marginal and poor, in order of increasing concentration[1]. In the good solvent regime, polymer chains are swollen and overwhelming binary interactions between segments prevail. In the marginal regime, chains are nearly ideal but slightly perturbed by the presence of binary and ternary interactions. Finally, in the theta regime, binary interactions vanish and the chains are essentially ideal with residual ternary interactions.

In the following we focus our attention on the marginal and theta regimes; in what follows we refer to the two regimes together as the poor solvent regime. The conditions of the poor solvent regime are[1,2]

$$\frac{\beta_1}{\rho b^6} < 1 \quad \text{and} \quad \frac{\beta_2}{b^6} < 1 \tag{1}$$

where $b^2$ is the mean square length of a polymer segment, $\beta_1$ and $\beta_2$ are the binary and ternary cluster integrals of

---

* To whom correspondence should be addressed

0032-3861/94/11/2284–06

segments, and $\rho$ is the number of polymer segments per unit volume of solution. In the semidilute poor solvent regime, as was first recognized by Edwards[3], the spatial fluctuation of the concentration of polymer segments is small, so that a mean field theory may be applied. Then the free energy density is[4,5]

$$F = kT\left[\left(\frac{\rho}{N}\right)\ln\rho + \frac{1}{2}\beta_1\rho^2 + \frac{1}{2}\beta_2\rho^3\right] \tag{2}$$

where $k$ is Boltzmann's constant, $T$ is the absolute temperature and $N$ is the number of segments in the polymer chain. In the case of a polydisperse system the first term on the right-hand side must be replaced by

$$kT\sum_i\left(\frac{\rho_i}{N_i}\right)\ln\rho_i$$

where $N_i$ and $\rho_i$ denote the respective quantities of the $i$th species.

The smallness of the spatial fluctuation of the segment density allows us to calculate the density–density correlation function of the polymer segments by a random phase approximation or its equivalent[6-9]. The Fourier transform $G(\mathbf{q})$ of the correlation function is obtained as

$$\frac{1}{G(\mathbf{q})} = \frac{1}{G_0(\mathbf{q})} + \beta_1 + 3\beta_2\rho \tag{3}$$

where $G_0(\mathbf{q})$ is the Fourier transform for a single chain. We are concerned with the so-called intermediate momentum range

$$\left(\frac{6}{Nb^2}\right)^{1/2} < q < \frac{1}{b} \tag{4}$$

then $G_0(\mathbf{q})$ can be written as

$$\frac{1}{G_0(\mathbf{q})} = \frac{b^2}{12}\left(q^2 + \frac{6}{Nb^2}\right) \tag{5}$$

and we obtain

$$G(\mathbf{q}) = \frac{12}{b^2}\,\frac{1}{q^2 + \xi^{-2}} \tag{6}$$

where the correlation length $\xi$ is given by

$$\xi^{-2} = \frac{6}{Nb^2} + \frac{12}{b^2}\beta_1\rho + \frac{36}{b^2}\beta_2\rho^2 \tag{7}$$

In place of the quantities associated with polymer segments, $N$, $b^2$, $\beta_1$, $\beta_2$ and $\rho$, we use measurable quantities, $M$, $A^2$, $B_1$, $B_2$ and $C$, defined as follows[8]

$$\begin{aligned} MA^2 &= Nb^2 \\ M^2B_1 &= N^2\beta_1 \\ M^3B_2 &= N^3\beta_2 \\ \frac{C}{M}N_A &= \frac{\rho}{N} \end{aligned} \tag{8}$$

where $M$ is the molecular weight of the polymer molecule, $N_A$ is Avogadro's number and $C$ is the weight concentration of the polymer.

The angular dependence of the scattered intensity $I(\mathbf{q})$, which is proportional to $G(\mathbf{q})$, is given by

$$I(\mathbf{q}) = \frac{I(\mathbf{0})}{1 + \xi^2q^2} \tag{9}$$

where

$$\xi^{-2} = \frac{6}{MA^2} + 12N_A\frac{B_1}{A^2}C + 36N_A^2\frac{B_2}{A^2}C^2 \tag{10}$$

The vector $\mathbf{q}$ is now the scattering wave vector $q = (4\pi/\lambda)\sin(\theta/2)$, where $\lambda$ is the wavelength of the incident neutrons and $\theta$ is the scattering angle. For a polydisperse system the latter equation must be replaced by

$$\xi^{-2} = \frac{6}{M_nA^2} + 12N_A\frac{B_1}{A^2}C + 36N_A^2\frac{B_2}{A^2}C^2 \tag{11}$$

where $M_n$ is the number-average molecular weight of the polymer. It has already been demonstrated[2,8,10] that equations (9), (10) and (11) work quite well for *UCST* systems such as a polystyrene–cyclohexane solution in the semidilute poor solvent regime.

In terms of the measurable quantities defined above the interaction part of the free energy density (the second and third terms of equation (2)) is expressed as

$$F_{\mathrm{int}} = N_AkT\left(\frac{1}{2}B_1N_AC^2 + \frac{1}{2}B_2N_A^2C^3\right) \tag{12}$$

## EXPERIMENTAL

### *Materials*

PVME ($M_n = 46\,500$, $M_w/M_n = 2.12$) was obtained from Scientific Polymer Products. The sample was freeze dried and stored in a vacuum box. Deuterium oxide ($D_2O$) (99.9 atom% deuterated) and deuterated methanol ($CD_3OD$) (99.5 atom% deuterated) were purchased from Aldrich. All solutions were prepared in sealed tubes. The concentrations of the solutions ranged from 0.06 g cm$^{-3}$ to 0.19 g cm$^{-3}$.

### *SANS measurements*

The measurements were performed with the KENS-SAN instrument at KEK (the National Laboratory for High Energy Physics at Tsukuba).

The instrument was installed on a pulsed cold neutron source and all wavelengths between 0.30 and 0.83 nm were used at the same time to increase the counting efficiency. The detector used was a two-dimensional position-sensitive detector (2D-PSD), composed of 43 one-dimensional position-sensitive counters, set at a distance of 3 m from the sample. The direct beam was focused on the centre of the detector by using a converging Soller slit. The intensity of the incident beam was $4\times10^4$ n s$^{-1}$ cm$^{-2}$ and the area of the cross-section of the beam at the sample was $14\times35$ mm$^2$. The sample cell was made of a pair of quartz windows 0.5 mm thick and the thickness of the sample solution was 2 mm.

The excess scattered intensity of the PVME solution compared with the solvent was determined after transmission correction was made both for solution and solvent. In order to compensate for the uniform incoherent scattering due to the hydrogen atoms we added water or normal methanol to the solvent so that the solvent and sample solution had the same number of protons.

The incident neutron spectrum and the detector efficiency of the 2D-PSD were corrected by using the incoherent scattering data from water.

The solvent compositions of the measured solutions were $D_2O$, $D_2O$ + 10 vol% $CD_3OD$ and $D_2O$ + 30 vol%

$CD_3OD$; these solutions are referred to respectively as system A, system 10 and system 30 in what follows. For each system several temperatures slightly below the phase separation temperature were chosen for the SANS measurement. These temperatures are summarized in *Table 1*. The temperature of the sample solution was controlled to within ±0.05°C.

## RESULTS

*Figure 1* shows the angular dependences of the scattered neutrons from the solution and the solvent; for the latter the scattering intensity is independe of $q$ in the measured small-angle range. In *Figure 2* the reciprocal of $I(\mathbf{q})$, the intensity of the excess scattering from the solution over the solvent, is plotted against $q^2$, demonstrating that the measured $I(\mathbf{q})$ obeys equation (9) for the condition $q^2 < 0.4\,\mathrm{nm}^{-2}$. From this figure we can determine the correlation length $\xi$ for each concentration and temperature. The concentration dependence of $\xi$ for each temperature turned out to agree well with the prediction of equation (11), as shown in *Figure 3*. Thus we were able to determine $B_1$ and $B_2$ separately as functions of temperature. In the course of the calculation we have assumed that the temperature dependence of $A$ is weak and used the reported[11] value $A = 0.09\,\mathrm{nm}$. *Figure 4* shows the temperature dependences of $B_1$ and $B_2$ thus obtained. Here we define Θ as the temperature at which $B_1$ vanishes. The values of Θ for the measured systems are listed in the second column of *Table 2*. In *Figure 5*

**Table 1** Temperatures of the SANS measurements. The *LCST* for each system is also shown

| System | Temperature (°C) | *LCST* (°C) |
|---|---|---|
| A: PVME–$D_2O$ | 23.5, 25.3, 26.5, 28.0, 30.1, 31.0, 32.5 | 34 |
| 10: PVME–($D_2O$ + 10 vol% $CD_3OD$) | 29.0, 31.0, 33.0, 35.0, 36.5 | 38 |
| 30: PVME–($D_2O$ + 30 vol% $CD_3OD$) | 40.0, 41.0, 42.0, 43.0 | 45 |

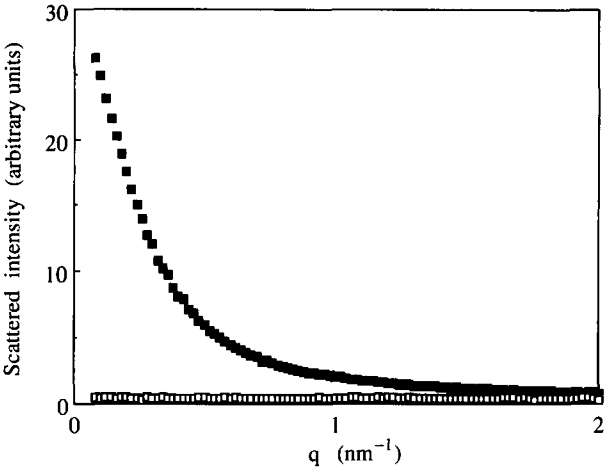

**Figure 1** Plots of the angular dependence of the scattering intensity at small angles (40.0°C): (□) solvent ($D_2O$ + 30 vol% $CD_3OD$); (■) solution ($C = 0.12\,\mathrm{g\,cm^{-3}}$)

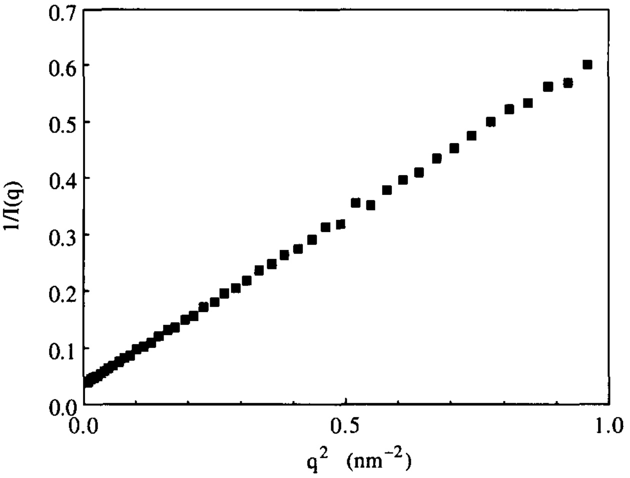

**Figure 2** Lorentzian plot of the excess scattering from solution for PVME–($D_2O$ + 30 vol% $CD_3OD$) (40.0°C, $C = 0.12\,\mathrm{g\,cm^{-3}}$)

**Table 2** Parameters Θ and $B_{10}$ of the systems studied. The entropy and enthalpy parameters deduced from $B_1$ are also shown

| System | Θ (K) | $10^{26}B_{10}$ ($\mathrm{cm^3}$) | $\frac{S_1}{C^2}$ ($\mathrm{J\,K^{-1}\,cm^{-3}(g\,cm^{-3})^{-2}}$) | $\frac{U_1}{C^2}$ ($\mathrm{J\,cm^{-3}(g\,cm^{-3})^{-2}}$) | $\frac{z}{k}\Delta s$ | $10^{20}z\Delta\varepsilon$ (J) |
|---|---|---|---|---|---|---|
| A: PVME–$D_2O$ | 304 | −6.6 | 0.17 | 50 | −8.1 | −3.2 |
| 10: PVME–($D_2O$ + 10 vol% $CD_3OD$) | 310 | −5.5 | 0.14 | 43 | −6.9 | −2.7 |
| 30: PVME–($D_2O$ + 30 vol% $CD_3OD$) | 316 | −4.6 | 0.12 | 36 | −5.8 | −2.3 |
| PVME–$C_6H_{12}$ | 315 | 2.8 | −0.070 | −22 | 2.7 | 1.4 |

**Table 3** $S_{\mathrm{int}}$ and $U_{\mathrm{int}}$ at $T = 310\,\mathrm{K}$, $C = 0.1\,\mathrm{g\,cm^{-3}}$

| | $S_{\mathrm{int}}$ | | $U_{\mathrm{int}}$ | |
|---|---|---|---|---|
| System | $S_1$ ($\mathrm{J\,K^{-1}\,cm^{-3}}$) | $S_2$ ($\mathrm{J\,K^{-1}\,cm^{-3}}$) | $U_1$ ($\mathrm{J\,cm^{-3}}$) | $U_2$ ($\mathrm{J\,cm^{-3}}$) |
| A: PVME–$D_2O$ | $1.7 \times 10^{-3}$ | $9.7 \times 10^{-5}$ | 0.50 | 0.031 |
| 10: PVME–($D_2O$ + 10 vol% $CD_3OD$) | $1.4 \times 10^{-3}$ | $8.3 \times 10^{-5}$ | 0.43 | 0.026 |
| 30: PVME–($D_2O$ + 30 vol% $CD_3OD$) | $1.2 \times 10^{-3}$ | $2.5 \times 10^{-5}$ | 0.36 | 0.0080 |

the values of $B_1$ are replotted against the reduced temperature $\tau$ defined by

$$\tau = 1 - \Theta T^{-1} \tag{13}$$

The parameter $B_1$ is directly proportional to $\tau$ in the measured temperature range

$$B_1 = B_{10}\tau \tag{14}$$

The values of $B_{10}$ are also listed in *Table 2.*

It is worth mentioning that the calculated values of $B_1$ and $B_2$ in fact satisfy the condition of the poor solvent regime, i.e. inequalities (1).

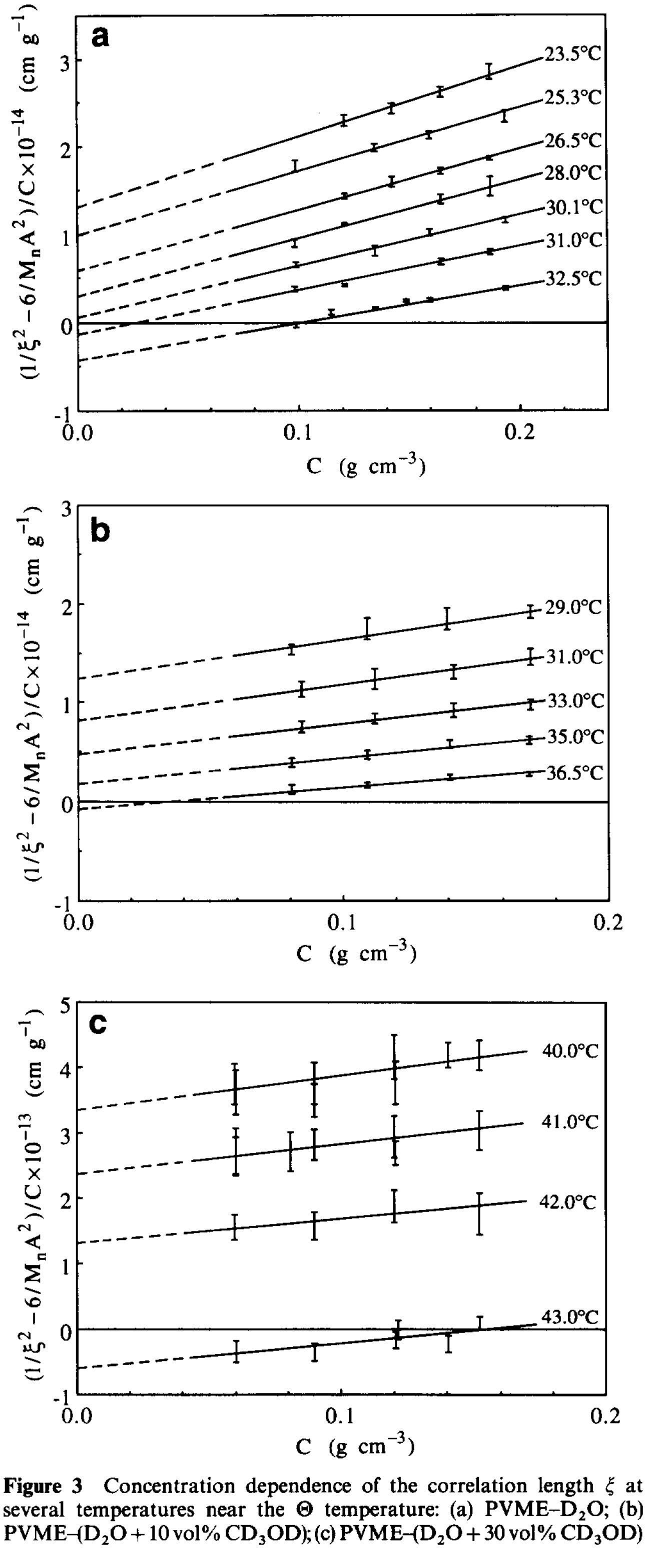

**Figure 3** Concentration dependence of the correlation length $\xi$ at several temperatures near the $\Theta$ temperature: (a) PVME–$D_2O$; (b) PVME–($D_2O$ + 10 vol% $CD_3OD$); (c) PVME–($D_2O$ + 30 vol% $CD_3OD$)

## DISCUSSION

The measured temperature dependences (*Figures 4a* and *4b*) of the interaction parameters $B_1$ and $B_2$ for the three systems studied here (PVME in an aqueous solvent (system A) and in water–alcohol mixtures (system 10 and system 30)) make a sharp contrast to those for PVME

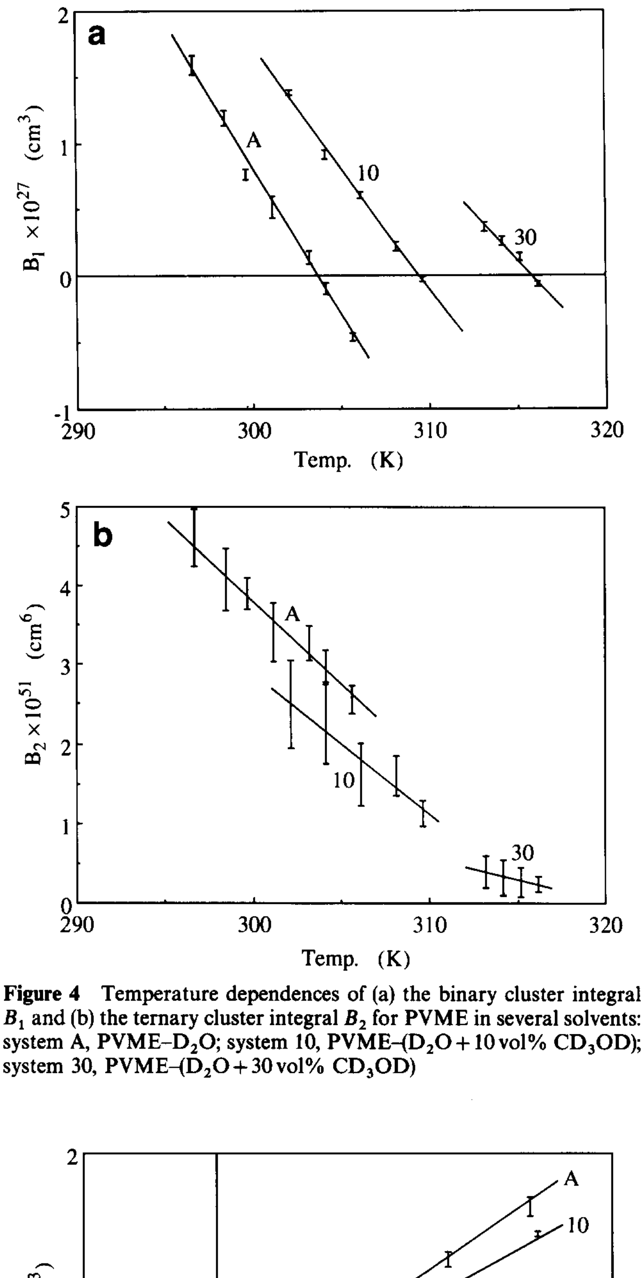

**Figure 4** Temperature dependences of (a) the binary cluster integral $B_1$ and (b) the ternary cluster integral $B_2$ for PVME in several solvents: system A, PVME–$D_2O$; system 10, PVME–($D_2O$ + 10 vol% $CD_3OD$); system 30, PVME–($D_2O$ + 30 vol% $CD_3OD$)

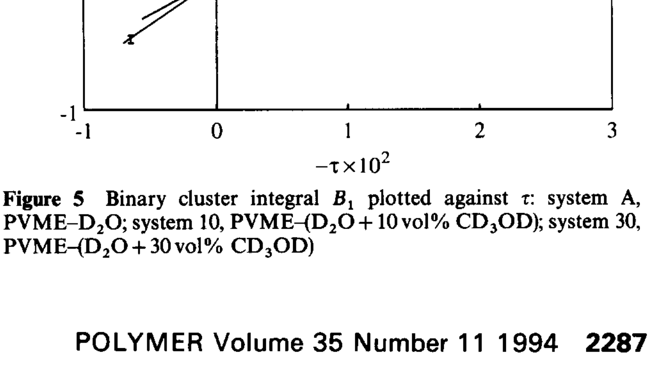

**Figure 5** Binary cluster integral $B_1$ plotted against $\tau$: system A, PVME–$D_2O$; system 10, PVME–($D_2O$ + 10 vol% $CD_3OD$); system 30, PVME–($D_2O$ + 30 vol% $CD_3OD$)

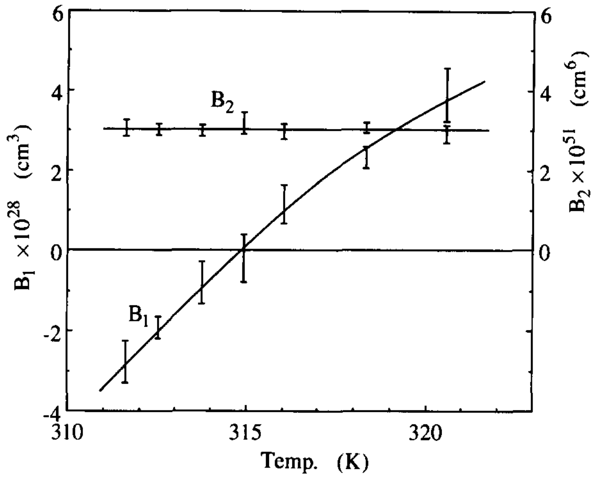

**Figure 6** Temperature dependences of the binary cluster integral $B_1$ and the ternary cluster integral $B_2$ for PVME in cyclohexane

in cyclohexane[12], which are reproduced in *Figure 6*. First, the temperature coefficient of $B_1$ is negative for the three systems studied here, while it is positive for the PVME–cyclohexane system. Second, $B_2$ for our three systems decreases rather sharply with temperature, while it is almost independent of temperature in cyclohexane.

In order to scrutinize this behaviour we have calculated for each system the contribution of the segment–segment interactions to the entropy $S_{\text{int}}$ and enthalpy $U_{\text{int}}$ from the measured temperature dependences of $B_1$ and $B_2$.

From the interaction part of the free energy density, equation (12), we obtain the equations for $S_{\text{int}}$ and $U_{\text{int}}$

$$S_{\text{int}} = -\frac{1}{2}N_A^2 k\left[\frac{\partial}{\partial T}(TB_1)C^2 + N_A\frac{\partial}{\partial T}(TB_2)C^3\right] \quad (15)$$

and

$$U_{\text{int}} = -\frac{1}{2}N_A^2 kT^2\left(\frac{\partial B_1}{\partial T}C^2 + N_A\frac{\partial B_2}{\partial T}C^3\right) \quad (16)$$

Let $S_1$ and $S_2$ denote respectively the first and second terms on the right-hand side of equation (15). Similarly, the first and second terms on the right-hand side of equation (16) are respectively denoted as $U_1$ and $U_2$. In particular, when the temperature dependence of $B_1$ is given by equations (13) and (14) we have

$$S_1 = -\frac{1}{2}N_A^2 kB_{10}C^2 \quad (17)$$

and

$$U_1 = -\frac{1}{2}N_A^2 kB_{10}\Theta C^2 \quad (18)$$

Using equations (15) and (16) we have calculated $S_{\text{int}}$ and $U_{\text{int}}$ from the measured temperature dependences of $B_1$ and $B_2$ for the three systems studied and found that they are both positive over the measured temperature and concentration ranges. In the PVME–cyclohexane system, however, $S_{\text{int}}$ and $U_{\text{int}}$ are both negative. *Table 3* gives examples of these values for the case $T = 310$ K and $C = 0.1$ g cm$^{-3}$, in the calculation of which the temperature dependences of $B_1$ and $B_2$ for system A and system 30 were extrapolated by about 5 K. We see that the values of $S_1$ and $U_1$ are larger by more than an order of magnitude than the respective values of $S_2$ and $U_2$. This turned out to hold for all the solutions we measured. Therefore, in the following, we focus our attention on $S_1$ and $U_1$.

In order to understand qualitatively the observed behaviour we invoke Flory's classical mean field theory, based on the latice model, as extended to include the entropy change associated with elementary interactions among solvent molecules and polymer segments[4,13]. To do so we regard a methanol–water mixture as an effective medium and we simply modify the usual $\chi$ parameter as

$$\chi = \frac{z}{kT}(\Delta\varepsilon - T\Delta s) \quad (19)$$

by taking into account the entropy change $\Delta s$ associated with the elementary interaction in addition to the associated enthalpy change $\Delta\varepsilon$. The parameter $z$ in equation (19) is the number of nearest-neighbour sites in the lattice. The theory predicts that when $N \gg 1$, the conditions for a *UCST* are

$$\Delta\varepsilon > 0 \quad \text{and} \quad 1 + \frac{2z}{k}\Delta s > 0 \quad (20)$$

while an *LCST* occurs if

$$\Delta\varepsilon < 0 \quad \text{and} \quad 1 + \frac{2z}{k}\Delta s < 0 \quad (21)$$

In the semidilute range the theory gives equation (12) together with

$$B_1 = B_{10}\left(1 - \frac{\Theta}{T}\right) \quad (22)$$

$$B_{10} = \left(1 + \frac{2z}{k}\Delta s\right)\frac{a^3}{m^2} \quad (23)$$

$$\Theta = \frac{\frac{2z}{k}\Delta\varepsilon}{1 + \frac{2z}{k}\Delta s} \quad (24)$$

and

$$B_2 = \frac{1}{3}\frac{a^6}{m^3} \quad (25)$$

where $m = M/N$ is the molecular weight of the segment and $a$ is the lattice constant. If the temperature dependences of $\Delta\varepsilon$ and $\Delta s$ are neglected, the contributions of the segment–segment interactions to the entropy $S_1$ and enthalpy $U_1$ can be expressed as

$$\frac{S_1}{C^2} = -\frac{1}{2}N_A^2 k\left(1 + \frac{2z}{k}\Delta s\right)\frac{a^3}{m^2} \quad (26)$$

$$\frac{U_1}{C^2} = -N_A^2 z\Delta\varepsilon\frac{a^3}{m^2} \quad (27)$$

The fourth and fifth columns of *Table 2* show the $S_1/C^2$ and $U_1/C^2$ calculated from the measured $\Theta$ and $B_{10}$ by using equations (17) and (18) for each system. We have also evaluated the corresponding values of $(z/k)\Delta s$ and $z\Delta\varepsilon$, which are shown in the last two columns of *Table 2*. In the calculation we have tentatively chosen the bond length of the backbone carbon atoms for the lattice constant $a$ and one half of the molecular weight of the repeat unit of PVME for $m$.

We see that in the framework of Flory's theory the measured temperature dependence of $B_1$ is consistent with the condition for the occurrence of an *LCST* (inequalities (21)). However, Flory's theory fails to explain the rather strong temperature dependence of $B_2$.

The properties $\Delta s<0$ and $\Delta\varepsilon<0$ can be understood quite easily if we consider hydrogen bonding between the ether groups of PVME and the ambient solvent molecules as well as hydrophobic hydration of the apolar groups of PVME[14,15]. We are not in a position to analyse these values in detail. However, in view of the fact that the strength[16] of a hydrogen bond is of the order of $10\,\mathrm{kJ\,mol^{-1}}$ and the angular fluctuation[17] of a hydrogen bond is restricted to about 10°, we may say that the estimated values of $z\Delta\varepsilon$ and $(z/k)\Delta s$ are not unreasonable.

The addition of methanol to the aqueous PVME solutions is expected to reduce the probabilities of occurrence for segment–solvent hydrogen bonding and hydrophobic hydration around the polymer segments. This may explain the systematic decreases in $S_1$ and $U_1$ with increasing methanol content.

## CONCLUSIONS

We measured the small-angle neutron scattering from semidilute solutions of PVME in water and in mixed methanol–water solvents, solutions that show an *LCST*, for various temperatures slightly below the phase separation temperatures. We found that the solutions studied are in the poor solvent regime and that the spatial correlation function of the segment concentration can be adequately described by the random phase approximation or its equivalent.

We determined the binary and ternary cluster integrals, $B_1$ and $B_2$, of the segments of PVME in water and in methanol–water mixtures as functions of temperatures. From the measured temperature dependences of these parameters we calculated the contributions of the segment–segment interactions to the entropy $S_{\mathrm{int}}$ and enthalpy $U_{\mathrm{int}}$ for aqueous and methanol–water solvents. It turned out that for all the systems both $S_{\mathrm{int}}$ and $U_{\mathrm{int}}$ were positive in the measured temperature range. We also found that the dominant contribution to $S_{\mathrm{int}}$ and $U_{\mathrm{int}}$ came from the binary interactions term $B_1$.

In order to understand qualitatively the implication of these findings we compared the above results with Flory's classical mean field theory for a two-component system in which the entropy change associated with the elementary segment–solvent, solvent–solvent and segment–segment interactions is taken into account. The theory shows that the observed temperature dependence of $B_1$ and the *LCST* behaviour are in fact consistent. In particular, the analysis demonstrated that the entropy and enthalpy changes associated with the elementary interactions, $\Delta s$ and $\Delta\varepsilon$, are negative, which, together with the decrease in the absolute values of these quantities with increasing methanol content, is in accord with the accepted picture of hydrogen bonding and hydrophobic hydration among polymer segments and solvent molecules[14,15]. The theory, however, cannot explain the observed strong temperature dependence of $B_2$. It is not possible at present to analyse these experimental findings more thoroughly, as the necessary theoretical background has yet to be developed.

## ACKNOWLEDGEMENTS

The authors thank KEK (the National Laboratory for High Energy Physics) for support and patience during the course of the many years of study. They are deeply indebted to Dr E. Wada for his encouragement and advice. Thanks are also tendered to Messrs T. Nakamura, S. Hirota, R. Murakami, A. Shizuno, Y. Ishihara and Y. Yoshimura for their earnest help in the SANS measurements.

## REFERENCES

1 Schaefer, D. W. *Polymer* 1984, **25**, 387

2 Okano, K., Ichimura, T., Kurita, K. and Wada, E. *Polymer* 1987, **28**, 693

3 Edwards, S. F. *Proc. Phys. Soc. London* 1966, **88**, 265

4 Flory, P. J. 'Principles of Polymer Chemistry', Cornell University Press, Ithaca, NY, 1953, p. 509

5 de Gennes, P. G. 'Scaling Concepts in Polymer Physics', Cornell University Press, Ithaca, NY, 1979, p. 73

6 Moore, M. A. *J. Physique* 1977, **38**, 265

7 Schaefer, D. W., Joany, J. F. and Pincus, P. *Macromolecules* 1980, **13**, 1280

8 Okano, K., Kurita, K., Nakajima, S., Wada, E., Furusaka, M. and Ishikawa, Y. *Physica B* 1983, **120**, 413

9 Benoit, H. and Benmouna, M. *Polymer* 1984, **25**, 1059

10 Ichimura, T., Okano, K., Kurita, K. and Wada, E. *Polymer* 1987, **28**, 1573

11 Manson, J. A. and Arquette, G. J. *Makromol. Chem.* 1960, **37**, 187

12 Takada, M., Okano, K. and Kurita, K. *Polym. J.* 1994, **26**, 113

13 Guggenheim, E. A. *Trans. Faraday Soc.* 1948, **44**, 1007

14 Franks, F. and Reid, D. S. in 'Water, A Comprehensive Treatise' (Ed. F. Franks), Vol. 2, Plenum Press, New York, 1973, pp. 323–380

15 Tanford, C. 'The Hydrophobic Effect', Wiley, New York, 1973, pp. 24–35

16 Israelachvili, J. N. 'Intermolecular and Surface Forces', Academic Press, London, 1985, p. 98

17 Walker, J. S. and Vause, C. A. *Sci. Am.* 1987, **256**(5), 90